CABLE SHEATH DIAGNOSIS IN CROSS BONDING CABLE SYSTEMS

Marina A. **SHOKRY**, Abderrahim **KHAMLICHI;** (UPM), (Spain); madel@lcoe.etsii.upm.es, ak@lcoe.etsii.upm.es,
Fernando **GARNACHO;** (LCOE-FFII), (Spain); fgarnacho@lcoe.etsii.upm.es
Julio **MARTÍNEZ;** (UPM), (Spain); julio.martinezm@upm.es,
Ángel **GONZALO**, Diego **PRIETO;** (UFD), (Spain); agonzaloc@ufd.es, dprieto@ufd.es
Jorge **ROVIRA;** (LCOE-FFII), (Spain); jrovira@lcoe.etsii.upm.es

ABSTRACT

On-line monitoring is now getting more focus on detecting defects in HV insulated cable system in order to prevent failures. Cross Bonding (CB) configurations are widely used in long power transmission land lines in order to reduce the circulating currents through cable metal sheath. This paper presents a general criterion for detecting defects in cable sheaths in CB configuration. Three types of defects are studied in this paper; open circuit fault in sheath loop, two phase short circuit in linkboxes (breakdown between sectionalized sheaths) and flooding in linkboxes. ATP software is used for the simulation of these defects on the modelled system. The criterion developed is studied on a real double circuit cable system in order to show the influence of varying the load of each one of the parallel lines. Real measurements have been performed on this cable system under normal condition; there is a good agreement between the measured and simulated results.

KEYWORDS

Condition monitoring, current measurements, electric breakdown, cable shielding, sheath current.

INTRODUCTION

On-line diagnostic techniques are gaining more focus by utilities, in order to save up the life time of insulated power cables. The main advantage of applying on-line monitoring for the assessment of the cable sheath condition is that the interruption of power supply is not required, while in off-line measurements a planned shutdown is needed [1-4].

The feasibility of detecting a fault in the cable over-sheath by monitoring the sheath currents to ground at the end of the cross-bonded sections is presented in [4]. A method has been developed by Mingzhen Li et al to detect and localize faults in CB configuration by monitoring sheath currents [2].

Different criteria (depending on the type of the defect) were developed by Xiang Dong et al. [1] to detect defects in cable sheaths by measuring sheath currents when CB configurations without transposition in flat formation are adopted.

In long underground cable systems, CB configuration or a combination between CB and Single Point (SP) are usually used [5-8]. Most cable systems are installed between two substations. Each substation may feed more than one underground transmission line so that there are more than one underground line connected in parallel and sharing some kilometres from the beginning substation. In this case, the load current applied on each of the connected lines may affect / have an influence on the other which certainly affects the sheath current at each measuring point.

This paper presents the application of the criterion developed in [9] on a real double circuit cable system. The criterion applied is based on simple codes from 0 to 4, representing the level of change in the cable sheath currents in case of defect. This paper studies the influence of changing the load current on each one of the parallel lines on the sheath current obtained at each measuring point on the two parallel lines. Real measurements have been performed under normal condition. There is a good agreement between the measured and simulated results.

PROBLEM STATMENT

The CB configuration as shown in Fig.1, consists of three minor sections. The cable sheaths of each minor section are interconnected together through linkboxes. The sheath current can be measured at four positions along the CB configuration at the terminal T_o and T_e and at linkboxes (LB_1 and LB_2). Sensors are fastened around unipolar cables at the terminals (I_o, I_e) while they are fastened around coaxial cables at linkboxes (I_1 and I_2).

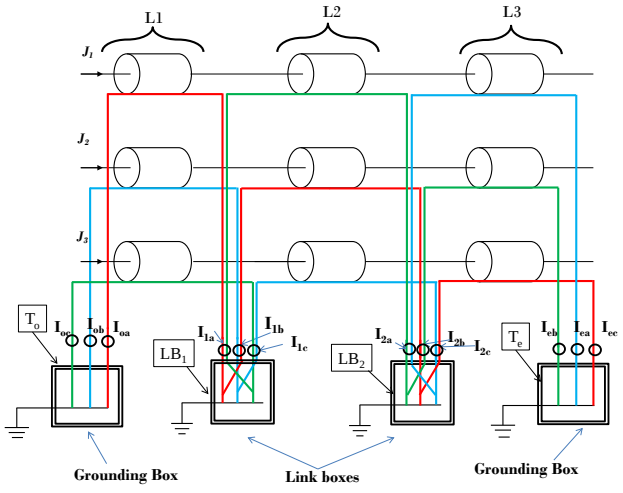

Fig. 1 CB configuration

Sensors at linkboxes (I_1 and I_2) are measuring the difference in the current between two sheath loops interconnected together. Sensors at the terminal (I_o and I_e) are measuring the current in one sheath loop. However in some practical situation where two CB are connected in series, the beginning terminal of one is interconnected to the other ending terminal through unipolar cables. In this situation, the measured current will be the subtraction of both.

In SP configuration, there is only one measuring point for the sheath current, where the measured current is the capacitive current as shown in Fig.2.

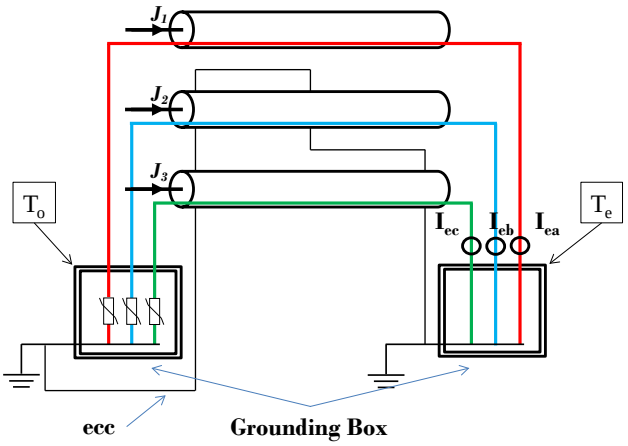

Fig. 2 SP configuration

Description of the circuit under analysis

The circuit consists of two parallel underground transmission lines. Both lines are sharing 1110m from the first substation. Line 1 consists of one major section of CB configuration while line 2 consists of two series SP configurations and two series CB configurations. Table 1 shows the parameter of the modelled cable on the ATP software. Fig. 3 shows the trenches of the sharing part of the circuit .The circuit has been modelled on ATP software as shown in Fig.4.

Table 1: Cable simulated parameters

Parameters	Value
Equivalent radius of the conductor (mm)	28
Equivalent relative permittivity of insulation	3.017
Equivalent external sheath raduis (mm)	53.8
Equivalent internal sheath raduis (mm)	52.5
Equivalent sheath resistivity at 80ºC (Ω·m)	4.785×10^{-8}
Equivalent conductor resistivity at 90ºC (Ω·m)	2×10^{-8}
Ground resistance (Ω)	0.2

As shown in Fig. 3, the formation type of the common part of both lines is a combination of trefoil and semi-trefoil formation while the remaining part of both line is in trefoil formation.

Sheath current under normal condition

The sheath current can be measured at 12 various points along the circuit as shown in table 2 and fig.4. For the sake of simplicity and due to the space limit, the results of only two points on each CB configuration are presented in this paper. In addition, the result of the common earth connection of two single point is presented. The sensors in which there results are presented in this paper are marked in red in table 2.

Table 2:Possible points of measurments

Line under measurements	Sensor	Location of the sensor on the circuit
Line 1	I_{o1}	Beginning terminal of line 1
	I_{j11}	LB1 of line 1
	I_{j21}	LB 2 of line 2
	I_{f11}	Ending terminal of line 2
Line 2	I_{f12}	Ending terminal of SP 1 and SP2 of line 2
	I_{o2}	Beginning terminal of CB1 of line 2
	I_{j12}	LB1 of CB1 of line 2
	I_{j22}	LB2 of CB1 of line 2
	I_{f22}	Ending terminal of CB1 and beginning terminal of CB2 of line2
	I_{j32}	LB1 of CB 2 of line 2
	I_{j42}	LB2 of CB 2 of line 2
	I_{f32}	Ending terminal of line 2

Table 3, 4 and 5 show the simulated sheath current at each of the indicated sensors corresponding to line 1 in table 2 corresponding to line 1 and line 2 when the load currents applied on both lines (Iload1 and Iload 2) are under the conditions stated in table 6.

Table 3: Calclated sheath current in line 1

Load current condition	I_{o1a} (A)	I_{o1b} (A)	I_{o1c} (A)	I_{j11a} (A)	I_{j11b} (A)	I_{j11c} (A)
Condition 1	8.96	15.2	2.30	34.4	25.6	12.4
Condition 2	10.9	10.2	4.30	31.3	17.4	14.8
Condition 3	2.36	5.17	4.12	17.9	14.4	6.61
Condition 4	1.78	6.34	3.90	18.7	16.6	7.09

Table 4: Calculated sheath current in line 2 in the second CB

Load current condition	I_{f22a} (A)	I_{f22b} (A)	I_{f22c} (A)	I_{j32a} (A)	I_{j32b} (A)	I_{j32c} (A)
Condition 1	102	104	100	148	148	146
Condition 2	10.1	9.18	8.35	22.2	22.1	22
Condition 3	24.9	25.2	23.9	43.6	43.3	43.1
Condition 4	50.2	51.3	49.2	78.1	77.6	77.9

Table 5: Calculated sheath current in line 2 in the first CB

Load current condition	I_{f12a}	I_{f12b}	I_{f12c}	I_{o2a}	I_{o2b}	I_{o2c}	I_{j12a}	I_{j12b}	I_{j12c}
Condition 1	0.3	0.3	0.3	118	118	112	207	207	146
Condition 2	0.3	0.3	0.3	13.4	13.4	12.7	27.9	27.7	27.6
Condition 3	0.3	0.3	0.3	30.9	30.9	29.4	58.3	58.0	57.6
Condition 4	0.3	0.3	0.3	59.5	59.5	59.6	107	106	105

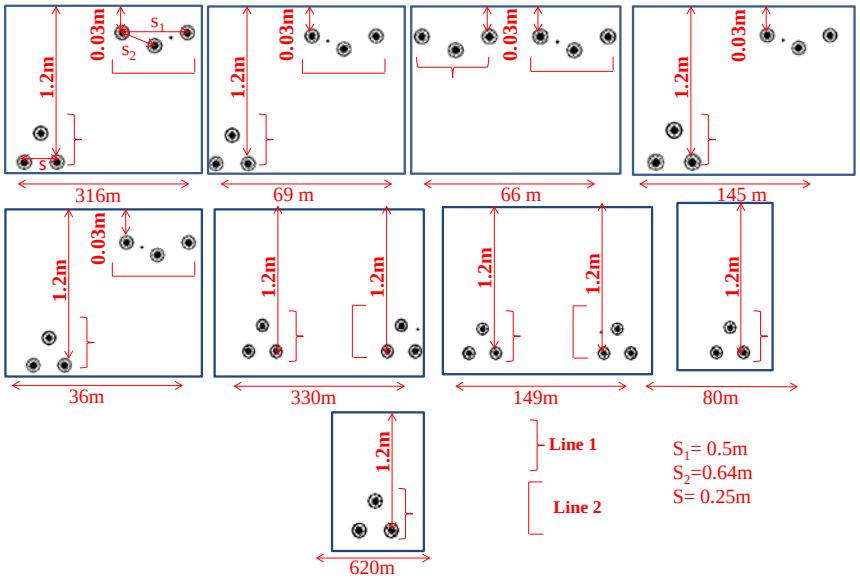

Fig.3: Trenches of the commen part between line 1 and line 2

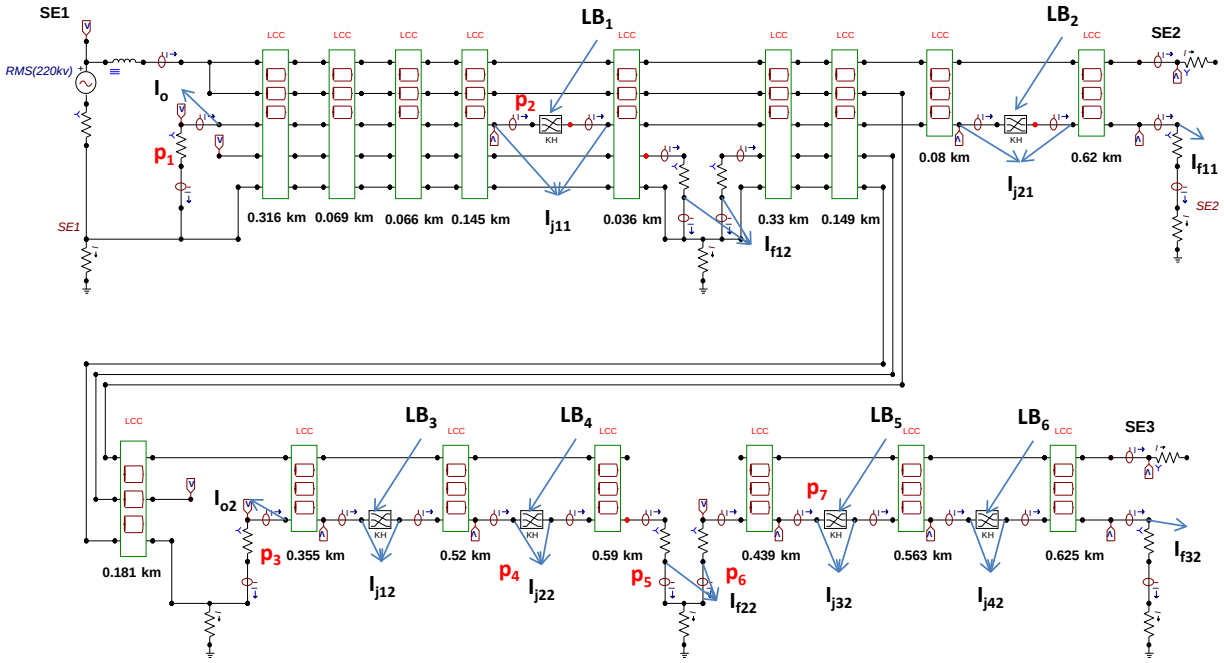

Fig. 4: Modeled circuit on ATP software

Table 6: Studied load current conditions

Condition1	I_{load1}=100% and I_{load2}= 100%
Condition2	I_{load1}=100% and I_{load2}= 10%
Condition3	I_{load1}=50% and I_{load2}= 25%
Condition4	I_{load1}=50% and I_{load2}= 50%

DETECTION CRITERION

A general criterion for detecting defects in cable sheath was introduced in [9] on the basis of the total induced current in the cable sheath (TICS). The TICS in each sensor is expressed in per-unit being referred to its expected value in the normal operation condition (no defect). The resulted values are classified into 4 discrete levels #0, #1, #2, #3 and #4 (see Table 6), each level represents a change in the sheath current (Is) in case of defect with respect to the expected current for normal operation (no defect).

Level #1 is used to represent the current level in normal conditions (no defect) with a tolerance of 25%, taking into account the influence parameters such as: percentage of unbalance in the minor sections, load current, cable characteristics, measuring uncertainties, temperature effect etc. Table 3,4 and 5 show the per-unit reference values of the cases studied in this paper.The transition limit between level #2 and #3 (7.5pu) and between #3 and #4 (12.5pu) are chosen with an order of magnitude greater (10 times) than the threshold to pass from #0 to #1 and from #1 to #2.

TYPE OF DEFECTS

This section is devoted to show different types of defects and the influence of these defects on the sheath current obtained from different sensors along the double circuit. The influence of changing the condition of load currents of both lines is also studied following the arrangement stated in table 7. The results are presented in function of the criterion explained in the above section. Where code 1 represents the level of change in sheath currents at sensors $I_{oa,b,c}$ and $I_{j11a,b,c}$,code 2 represents the level of change in the sheath currents of sensors $I_{f12a,b,c}$, $I_{o2a,b,c}$ and $I_{j12a,b,c}$ and code 3 represents the level of change in sensors $I_{f22a,b,c}$ and $I_{j32a,b,c}$.

It is important to note that, if the defect occurs on one of the parallel line, the other parallel line will not be affected, i.e. there will be no change in the sheath current of the other line. For this reason, only code 1 is presented when the defect occurs in line 1 and only code 2 and 3 are presented when the defect occurs in line 2.

Open circuit fault in sheath loop

Due to corrosion, poor installation or third party damage, a disconnection might occur between the sheath and ground. This defect has been simulated at different location along the double circuit in sheath a as shown in fig. 4. Tables 8 and 9 show the codes obtained when the disconnection occurs at different position on line1 and line 2 at different load current conditions. The positions of disconnection points are marked by “p” in fig.4.

Table 7: Obtained codes at different positions along line 1

Position		Code1
Position1	Condition1	002,011
	Condition2	001,010
	Condition3-4	011,111
Position 2	Condition1	002,011
	Condition2	002,010
	Condition3-4	202,011

As in the case of open circuit in sheath loop, the measured sheath current is only the capacitive current as well as in case of small percentage of unbalance in the minor sections as in the case of line 1. This leads to unchanged in the cable sheath current at the sensors in the linkboxes under certain conditions of load current (condition 3 and 4 in table 8). In these particular situations, the sensors have to be located at least at two measuring points (one at a terminal and the other at a linkbox).

Table 8: Obtained codes at different positions along line 2

Position		Code 2	Code 2
Position 3	Condition 1, 3-6	111,011,010	210,111
	Condition 2	111,001,010	
Position 4	Condition 1, 3-6	111,101,001	021,111
	Condition 2	111,100,101	
Position 5	Condition 1, 3-6	111,110,100	101,111
	Condition 2	111,100,101	102,111
Position 6,7	Condition 1-6	111,111,111	120,010

From table 9, it is noticed that the defect of open circuit fault in sheath loop can be detected by measuring the sheath current at only one point. This is due to the greater percentage of unbalance in the minor sections. Also there is a stability of the obtained cods under different conditions of load current except in condition 2 where the load current applied on line 2 is 10% of the rated current. This can be resolved by applying the capacitive current subtraction method stated in [9].

Breakdown between sectionalized sheaths or 2 phase short circuit in linkboxes

A failure in the insulation of the coaxial cables at the joints of a CB configuration, a failure in the insulation of the joints, a failure in the insulating flange between metal sheaths or a short circuit in the surge voltage limiters may cause a breakdown between two sectionalized sheaths or a short circuit between two phases of metal sheaths. These defects have been simulated by ATP software by connecting a very small resistance between two sectionalized sheaths in each linkbox or between two phase metal sheaths. It is observed that both defects are electrically the same. Due to the space limit, this defect has been simulated between sectionalized sheaths of phase a in case of breakdown between sectionalized sheaths and between the metal sheaths of phase a and b in case of 2 phase short circuit.Tables 8 and 9 show the codes obtained when the these defect occur in different linkboxes in line1 and line 2 under different load current

conditions. These two defects are considered electrically the same and produce exactly the same codes.

Table 9: Obtained code at different linkboxes along line 1

Position		Code1
LB1	Condition 1-4	441,344
LB 2	Condition 1-4	144,344

Table 10: Obtained code at different linkboxes along line 2

Position		Code2	Code 3
LB3	Condition 1-4	111,221,222	122,111
LB 4	Condition 1-4	111,122,221	212,111
LB 5	Condition 1-4	111,111,111	231,212
LB 6	Condition 1-4	111,111,111	122,222

From tables 10 and 11, it is noticed that these defects cause an increase in the sheath current which leads to codes formed of 4, 3 and 1 in line 1 and codes formed of 2, 3 and 1 in line 2. The difference in the codes produced when the defect is in line1 or line 2 is due to the difference in the percentage of unbalance in both lines. Different codes are obtained according to the location of the defect which facilitates the localization of the defect. It is important to note as well that the codes maintain stability under different conditions of load current. The current measured by sensor I_{f12} is not affected by any defect, as it is located at the ending of two single points.

Flooding in linkboxes

When the linkboxes are immersed in water due to excessive rain, flooding in linkboxes occurs. This leads to a three phase short circuit. This defect has been simulated at each linkbox of the studied double circuit. Tables 12 and 13 show the codes obtained when the flooding occurs in different linkboxes on line1 and line 2 at different load current conditions

Table 11: Obtained code at different linkboxes along line 1

Position		Code1
LB1	Condition1-4	444,444
LB 2	Condition1-4	444,444

Table 12: Obtained code at different linkboxes along line 2

Position		Code2	Code3
LB3	Condition1-4	111,222,222	222,111
LB 4	Condition1,3,4	111,222,222	222,111
	Condition2	111,222,222	233,111
LB 5	Condition1-4	111,111,111	333,222
LB 6	Condition1-4	111,111,111	333,322

It is observed from tables 12 and 13, that the flooding in linkboxes causes an excessive increase in the sheath current which leads to codes formed of all 4 in line 1 and codes formed of all 2 and all 3 in line 2.Different codes are produced according to the location of the defect (in which line and in which CB in the line). This facilitates the detection and the localization of the defect. Also, it should be noted that the code maintains stability at different conditions of load current. The current measured by sensor I_{f12} is not affected by any defect, as it is located at the ending of two single points.

MEASUREMENTS VALIDATION RESULTS

Real measurements were performed on the 4th of December 2018. The sensors were located around the coaxial cables at the exit of both linkboxes of line 1, as shown in Fig.5. The measurements of sheath currents in both linkboxes were synchronized with the measurements of the load currents of the two parallel lines.

Fig. 5: Sheath current measurments at LB1 of line 1

Table 14 shows the simulated and measured results. From Table 14 , it is observed that the cable is working under normal operation (with no defect detected). Also there is a good agreement between the measured and simulated results. It is important to note that for analyzing the measurements compatibility, the uncertainty of simulation should be also considered. The terminals have been checked in order to assure that there is no open circuit fault at the terminals.

Table 13: Measurments and simulation of sheath currents at LBs of line 1

Sensor (A)	$I_{Load\ 1}$	$I_{Load\ 2}$	I_{j11a}	I_{j11b}	I_{j11c}	I_{2a}	I_{2b}	I_{2c}
Measurement ± uncertainity	~450 ±4.6	~330 ±3.4	15.8 ±1.3	11.2 ±1.2	5.3 ±1.1	6.2 ±1.1	9.1 ±1.1	14.2 ±1.3
Simulation	450	330	14.8	13.5	6.2	6.2	8.6	13

CONCLUSION

This paper presents a generic method for detecting and localizing of defects in cable sheaths by measuring the cable sheath currents in HV cable systems of CB configurations. The paper studies three types of defects that might occur in a CB configuration; open circuit fault in sheath loop, breakdown between sectionalized sheaths or two phase short circuit between metal sheaths and flooding in linkboxes. The criterion developed is applied on areal double circuit cable system. It is noted that when the defect occurs in one line the other line is not affected. The codes developed in the paper can detect and localize defects in cable sheath with a certain stability of codes under 4 different load conditions. Measurements have been performed on part of the studied circuit; a good agreement is achieved between the measured and simulated results.

ACKNOWLEDGEMENT

This work has received funding from the European Union's Horizon 2020 research and innovation programme under the Marie Sklodowska-Curie grant agreement No 676042.

REFERENCES

[1] X. Dong, Y. Yang, C. Zhou and D. Hepburn, "Online Monitoring and Diagnosis of HV Cable Faults by Sheath System Currents", *IEEE Transactions on Power Delivery*, vol. 32, no. 5, pp. 2281-2290, 2017.

[2] Mingzhen Li, W. Zhou, Chunlin Wang, Leiming Yao, Mengting Su, Xiaojun Huang and C. Zhou, "A novel fault localization method based on monitoring of sheath current in a cross-bonded HV cable system", *2017 IEEE Electrical Insulation Conference (EIC)*, 2017.

[3] Y. Yang, D. Hepburn, C. Zhou, W. Zhou and Y. Bao, "On-line monitoring of relative dielectric losses in cross-bonded cables using sheath currents", *IEEE Transactions on Dielectrics and Electrical Insulation*, vol. 24, no. 5, pp. 2677-2685, 2017.

[4] M. Marzinotto and G. Mazzanti, "The Feasibility of Cable Sheath Fault Detection by Monitoring Sheath-to-Ground Currents at the Ends of Cross-Bonding Sections", *IEEE Transactions on Industry Applications*, vol. 51, no. 6, pp. 5376-5384, 2015.

[5] 575-2014 IEEE Guide for Bonding Shields and Sheaths of Single-conductor Power Cables Rated 5 Kv through 500 Kv. (2014).

[6] R. Benato, S. Dambone Sessa, R. De Zan, M. Guarniere, G. Lavecchia and P. Sylos Labini, "Different Bonding Types of Scilla–Villafranca (Sicily–Calabria) 43-km Double-Circuit AC 380-kV Submarine–Land Cables", *IEEE Transactions on Industry Applications*, vol. 51, no. 6, pp. 5050-5057, 2015.

[7] P. Simón Comín and F. Garnacho, *Cálculo y diseño de líneas eléctricas de alta tensión*. Madrid: Ibergarceta, 2011.

[8] A. Khamlichi, M. Adel, F. Garnacho and J. Rovira, "Measuring cable sheath currents to detect defects in cable sheath connections", *52nd International Universities Power Engineering Conference* (UPEC), 2017.

[9] M. Shokry, A. Khamlichi, F. Garnacho, J. Malo and F. Alvarez, "Detection and localization of defects in cable sheath of cross-bonding configuration by sheath currents", IEEE Transactions on Power Delivery, pp. 1-1, 2019. Available: 10.1109/tpwrd.2019.2903329.